Proton NMR Sequence-Specific Assignments and Secondary Structure of a Receptor Binding Domain of Mouse γ-Interferon†

Ted T. Sakai, Michael J. Jablonsky, Paul A. DeMuth, and N. Rama Krishna*

Comprehensive Cancer Center and Department of Biochemistry, University of Alabama at Birmingham, Birmingham, Alabama 35294

Michael A. Jarpe‡ and Howard M. Johnson

Department of Microbiology and Cell Science, University of Florida, Gainesville, Florida 32611

Received December 15, 1992; Revised Manuscript Received March 17, 1993

ABSTRACT: Previous studies using synthetic peptides and monoclonal antibodies have implicated the N-terminal 39-residue segment as a receptor binding region of mouse γ-interferon (MuIFNγ). In this work, we report the solution structure of this fragment (dissolved in water with 40% trifluoroethanol) as determined by proton NMR spectroscopy. The proton sequence-specific assignments were determined from TOCSY and NOESY spectra using established procedures. The secondary structure is characterized by two well-defined α-helical regions composed of residues 5–16 and 22–37. These two helices are joined by a loop. No NOESY contacts between the two helical regions were detected. Molecular models consistent with the NMR data were generated for MuIFNγ(1–39) using distance geometry and restrained molecular dynamics/energy minimization calculations. Comparison with similar N-terminal domains in the published NMR and crystallographic studies on the dimeric human and rabbit IFNγ suggests some similarities in the structures except that the helical regions in the fragment are longer, and considerable variation may exist in the relative orientation of the two helices in the solution phase. The presence of stronger αN sequential NOE's suggests that this peptide is flexible. The absence of NOESY contacts involving the N-terminal tripeptide suggests that this region undergoes rapid segmental motion. The data presented here on MuIFNγ(1–39), combined with the studies on human and rabbit IFNγ, suggest that the N-terminal receptor binding domain of the protein can undergo structural changes, the understanding of which may provide insight into the basis for receptor interaction by this lymphokine.

γ-Interferon (IFNγ)[1] is a glycoprotein involved in the initiation and regulation of the immune response (Johnson, 1985). Some of its functions are regulation of major histocompatibility complex antigen expression, B-cell maturation, antibody production, and activation of host defense against tumor cells and microorganisms (Vilcek et al., 1985). The crystal structures of human γ-interferon (Ealick et al., 1991) and rabbit IFNγ (Samudzi et al., 1991) in their dimeric forms have been reported. These two crystallographic structures show substantial differences in the definition of some of the α-helical segments, even though the overall folding patterns are similar. NMR assignments on a recombinant ^{13}C- and ^{15}N-labeled human IFNγ have also been reported more recently (Grzesiek et al., 1992).

As part of a program aimed at defining the mechanism of action of this protein and its mode of interaction with its receptor, a number of peptides representing different regions of the native murine protein have been synthesized (Griggs et al., 1992; Jarpe & Johnson, 1990; Magazine & Johnson, 1991). From a comparison of the abilities of the different synthetic peptides to compete with the intact protein in blocking IFNγ–receptor interaction, one of the receptor binding regions of the protein was identified as being located in the N-terminus of the molecule. Specifically, the synthetic 39-residue N-terminal fragment [MuIFNγ(1–39)] from the mouse protein was shown to inhibit IFNγ function and receptor binding (Magazine & Johnson, 1991; Magazine et al., 1988). Additionally, direct binding was demonstrated between MuIFNγ-(1–39) and the mouse receptor (Griggs et al., 1992). Of particular interest was the finding that the MuIFNγ(1–39) possesses a 10-fold greater ability to block human IFNγ antiviral activity and receptor binding than the corresponding fragment, HuIFNγ(1–39), from the human protein (Jarpe & Johnson, 1993). Based on a study of various monosubstituted analogues of MuIFNγ(1–39), residues 3, 4, and 14 and some residues in the 32–39 stretch were implicated in interaction of the fragment with receptor (Magazine & Johnson, 1991).

Circular dichroism measurements have been performed on different N-terminal fragments in water and water/trifluoroethanol (TFE) mixtures (Magazine & Johnson, 1991). The fragments examined were 1–39, 3–39, 5–39, 7–39, and 1–31 as well as 1–39 analogues with substitutions at positions 6, 8, and 14. MuIFNγ(1–39) exhibited some degree of α-helical structure in water, but the helical content was found to be maximal in a mixture of water and TFE (40% by volume),

† This work was supported by Grant MCB-9118503 from the National Science Foundation and by Grants CA-13148 and CA-38587 from the National Institutes of Health.

* Address correspondence to this author.

‡ Present address: Department of Physiology and Biophysics, University of Alabama at Birmingham.

[1] Abbreviations: IFN, interferon; IFNγ, interferon-γ; MuIFNγ(1–39), peptide consisting of residues 1–39 of murine interferon-γ; NMR, nuclear magnetic resonance; NOE, nuclear Overhauser effect; NOESY, nuclear Overhauser effect spectroscopy; COSY, correlation spectroscopy; DQF-COSY, double-quantum-filtered correlation spectroscopy; TOCSY, total correlation spectroscopy; CD, circular dichroism; TPPI, time-proportional phase incrementation; DSS, sodium 2,2-dimethyl-2-silapentane-5-sulfonate; TFE, 2,2,2-trifluoroethanol; TFE-d_3, 1,1,1-trideuterio-2,2,2-trifluoroethanol; CSI, chemical shift index; MD, molecular dynamics; EM, energy minimization.

0006-2960/93/0432-5650$04.00/0

a solvent known to stabilize helices. The present investigation is aimed at characterizing the solution structure of MuIFNγ-(1–39), the N-terminal receptor binding domain of the protein, by high-field NMR spectroscopy. Structural analysis of the receptor binding regions or domains is a prerequisite in the detailed elucidation of the structure–function relationships and in our understanding of the mode of action of IFNγ.

MATERIALS AND METHODS

The peptide was synthesized as described (Magazine & Johnson, 1991). Because the peptide aggregates in water at concentrations needed for NMR measurements, all NMR measurements were performed on a sample (0.9 mM) dissolved in a 60:40 mixture of H_2O/trifluoroethanol-d_3 (TFE-d_3). The pH of the solution was adjusted to 4.0 (meter reading). The NMR measurements were performed at 303 K on a Bruker AM-600 spectrometer operating in the quadrature detection mode. Three different NOESY (Macura & Ernst, 1980) data files were acquired in the TPPI mode (Marion & Wuthrich, 1983) with mixing times of 150, 300, and 450 ms. The time domain data size was typically 2K points in the t_2 domain with 512 t_1 increments. Two separate TOCSY experiments (Bax & Davis, 1985) with spin-lock times of 27 and 70 ms as well as a DQF-COSY experiment (Rance et al., 1983) were performed. The data size was 512 t_1 × 2K t_2 points for the TOCSY and 1024 t_1 × 4K t_2 for the DQF-COSY. The carrier frequency was centered on the H_2O resonance. Interference from the strong solvent resonance was minimized by presaturation during the preparation period (and during the mixing time for the NOESY). The data were transferred to a Silicon Graphics Indigo work station and processed using the program FELIX (Hare Research Inc., Bothell, WA). For the DQF-COSY data, the final digital resolution after zero-filling was 1.77 Hz/point in the ω_2 direction. Chemical shifts were expressed with respect to internal DSS (sodium 2,2-dimethyl-2-silapentane-5-sulfonate).

The molecular modeling calculations were performed on a Silicon Graphics IRIS Indigo work station using the XPLOR/QUANTA/CHARMm modeling package (Molecular Simulations, Inc., Burlington, MA). The modeling protocol used was identical to the one used by our laboratory in the study of other proteins (W. T. Lee, D. D. Watt, and N. R. Krishna, submitted for publication), and is based on the hybrid distance geometry/dynamical simulated annealing protocol described by Driscoll et al. (1989). Experimentally generated distance constraints derived from NOE intensities and torsion angle constraints derived from coupling constant information were used during restrained molecular dynamics and restrained energy minimization calculations. On the basis of cross-peak intensities in the NOESY spectra, recorded with mixing times of 150 and 300 ms, the NOE distance constraints were classified as strong (1.8–2.5 Å), medium (1.8–3.3 Å), and weak (1.8–5.0 Å). For residues with $^3J_{N\alpha} > 8$ Hz, ϕ was constrained to $-120° \pm 50°$; for residues with $^3J_{N\alpha} < 6.5$ Hz, ϕ was constrained to $-55° \pm 45°$. A total of 283 NOESY constraints and 32 backbone torsion angle constraints were used in generating structures using X-PLOR. The hydrogen bond constraints inferred in the two helical segments were also included.

RESULTS AND DISCUSSION

Assignment of Proton Resonances. The proton resonances were assigned to specific amino acids in the sequence using standard sequential assignment procedures (Wuthrich, 1986).

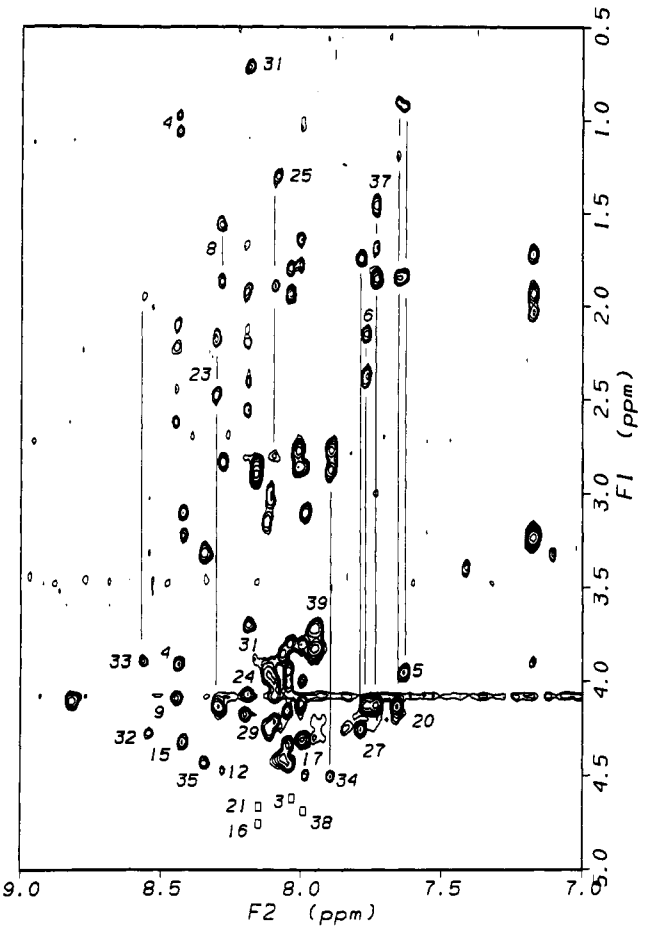

FIGURE 1: Amide proton region in the TOCSY spectrum of MuIFNγ-(1–39) [0.9 mM in a 60/40 (v/v) mixture of water/TFE-d_6, pH 4, 303 K]. Only some of the assignments are indicated in the spectrum. The squares represent the positions of N*H*–C$^{\alpha}$*H* cross-peaks for residues 3, 16, 21, and 38. Even though they are not apparent in this region of the spectrum, they were observed in the symmetric part of the TOCSY spectrum (not shown), and in the NOESY spectrum.

The TOCSY spectra were used to identify the peaks in the fingerprint region (N*H*–C$^{\alpha}$*H*) according to amino acid types. The sequential connectivities between the amino acids were traced out by following $d_{\alpha N}$, d_{NN}, and $d_{\beta N}$ connectivities. Some useful starting points in tracing connectivities were provided by the two valines, the lone arginine, and the aromatic ring systems. The cis and trans primary amide protons of Asn and Gln residues were identified from the strong cross-peaks due to cis/trans exchange and NOE (Krishna et al., 1982). These primary amide protons showed NOE contacts to their respective C$^{\beta}$H or C$^{\gamma}$H hydrogens. Figure 1 shows the 70-ms TOCSY spectrum of MuIFNγ(1–39) with most of the peaks in the fingerprint region identified. The sequential connectivities observed for this peptide are shown in Figure 2, and the sequence-specific chemical shift assignments are listed in Table I.

Conformational Features from NMR Data. (a) NOESY Connectivities. Figure 2 shows the sequential NOESY connectivities observed in MuIFNγ(1–39). Of particular interest are the $d_{NN(i,i+1)}$, $d_{\alpha N(i,i+3)}$, and $d_{\alpha\beta(i,i+3)}$ connectivities observed in two separate stretches, viz., residues 5–16 and 22–38. These connectivities unequivocally establish the presence of two separate α-helical regions in MuIFNγ(1–39). The d_{NN} connectivities are interrupted at residue 17; however, 17–21 show $d_{\alpha N}$ connectivities. Residues 19, 20, and 21 show d_{NN} connectivities as well as $d_{\alpha N}$ connectivities. However, these connectivities ($d_{\alpha N}$ and d_{NN}) are interrupted

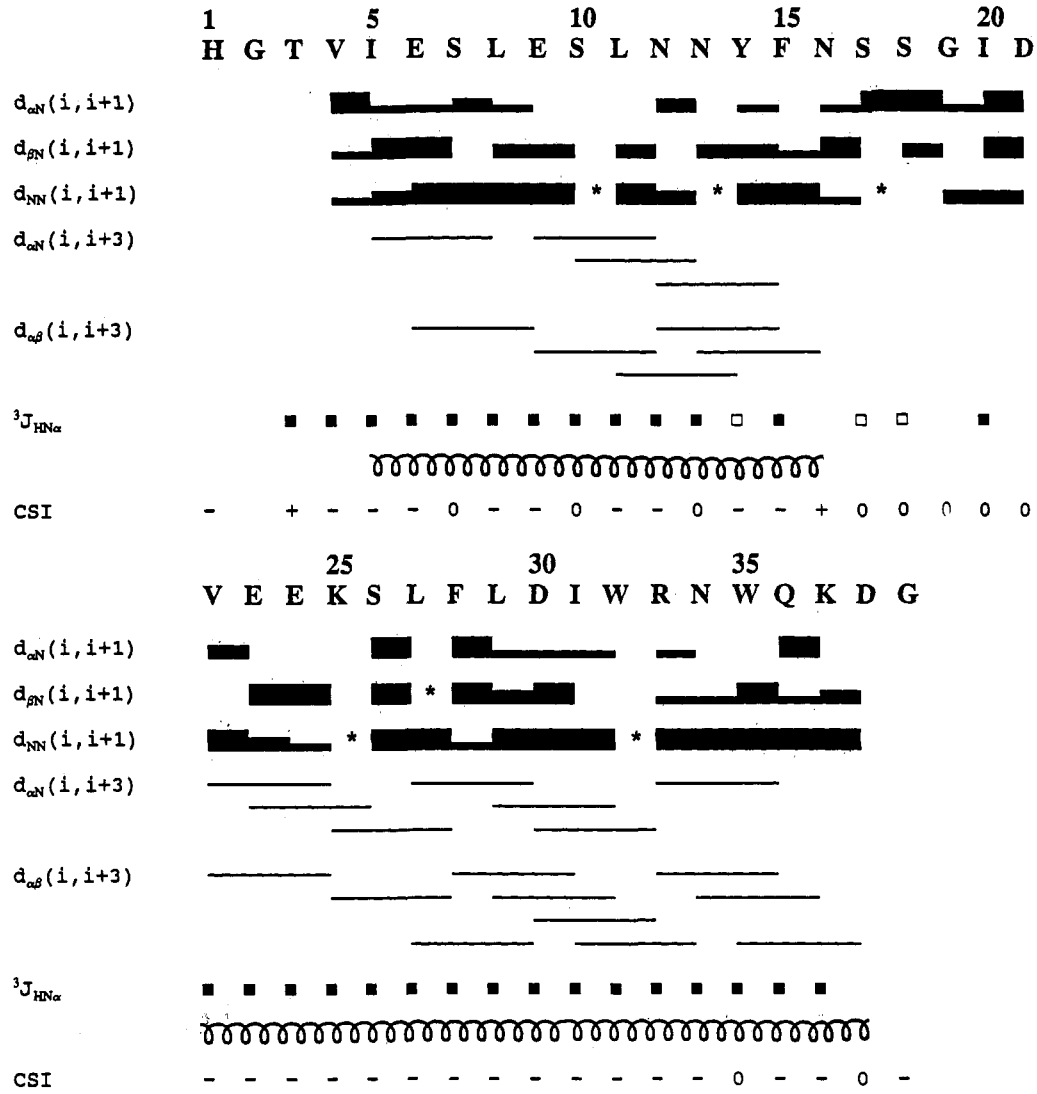

FIGURE 2: Sequential connectivity diagram for MuIFNγ(1–39) showing the (*i*,*i*+1) and (*i*,*i*+3) contacts observed in the NOESY spectra. The thickness of the bars for the (*i*,*i*+1) connectivities represents strong, medium, and weak intensities and were deduced from the NOESY spectra recorded with mixing times of 150 and 300 ms. No attempt was made to similarly quantitate the (*i*,*i*+3) connectivities. The asterisks indicate lack of information due to resonance overlap. Also shown in the figure are N*H*–C$^{\alpha}$*H* vicinal coupling constant data with filled squares representing coupling constants less than or equal to 6 Hz and open squares representing 7 Hz of larger values. The helical ergions 5–16 and 22–38 are also schematically shown. The CSI row represents the chemical shift index (Wishart et al., 1992), and was calculated using the "coil" values from Table 6 of Wishart et al. (1991). See the text for further discussion on calculating the CSI values.

at residue 21. These observations suggest a turn at residues 19 and 20 preceded by a short strand involving residues 17–19. The d_{NN} connectivities, together with the medium-range contacts [$d_{\alpha N(i,i+3)}$ and $d_{\alpha\beta(i,i+3)}$], commence again at residue 22, indicative of the beginning of the second helical region. Thus, the secondary structure inferred from the short- and medium-range NOESY contacts is that of a peptide with two α-helical regions separated by a short loop and a turn. The d_{NN} connectivities from the two α-helical regions are shown in the amide proton NOESY spectrum in Figure 3.

(*b*) *Vicinal NH–C$^{\alpha}$H Coupling Constants.* The backbone NH–C$^{\alpha}$H vicinal proton coupling constants were measured from DQF-COSY spectra for most of the resolvable peaks in the fingerprint region. The results are included in Figure 2, with open squares for coupling constants greater than 7 Hz and closed squares for coupling constants less than or equal to 6 Hz. The observed vicinal coupling constant data are consistent with the secondary structural conclusions deduced from the previous section using NOESY contacts, viz., two separate α-helix regions involving residues 4–16 and 22–38 separated by a loop involving residues 17–21.

(*c*) *Chemical Shifts of C$^{\alpha}$H and Amide Protons.* The analysis of chemical shifts of proteins to infer secondary structural features has long been a major goal of biomolecular NMR spectroscopists [e.g., see Perkins (1982) and Wagner et al. (1983)]. More recently, there has been a renewed interest in the possibility of using the deviations of chemical shifts of nuclei from the corresponding random-coil values as indicators of secondary structural elements in proteins (Wishart et al., 1991, 1992; Zhou et al., 1992). Figure 2 shows the chemical shift indexes (CSI) deduced for MuIFNγ(1–39). These indexes are a digitized version of the difference between the observed and coil chemical shift values for the C$^{\alpha}$H protons. On the basis of the criteria established by Wishart et al., the peptide is characterized by an α-helix composed of residues 4–16. This helix is interrupted at residue 16, as indicated by the change in the sign of the CSI. It commences again at residue 22 and continues up to residue 38. We should point out that in deducing the CSI values, we used the "coil" values for the reference chemical shifts [Table 6 in Wishart et al. (1991)] rather than the random-coil values in Table II of Wishart et al. (1992). The latter are more reflective of the

Table I: ^{1}H Resonance Assignments of the Individual Residues in the Murine γ-Interferon Peptide 1–39[a]

residue	NH	CαH	CβH	others	residue	NH	CαH	CβH	others
His-1		4.35	3.39	2H 8.55	Ser-26	8.09	4.21	3.97, 4.07	
				4H 7.40	Leu-27	7.78	4.24	1.73	CγH 1.68
Gly-2									CδH$_3$ 0.88, 0.94
Thr-3	8.08	4.60	4.47	CγH$_3$ 1.30	Phe-28	8.12	4.23	3.15	2,6H 7.15
Val-4	8.44	3.90	2.09	CγH$_3$ 0.97, 1.06					3,5H 7.07
Ile-5	7.63	3.94	1.84	CγH$_2$ 1.53					4H 7.10
				CγH$_3$ 0.93	Leu-29	8.20	4.17	1.92	CγH 1.67
				CδH$_3$ 1.29					CδH$_3$ 0.93, 0.96
Glu-6	7.76	4.12	2.14	CγH$_2$ 2.37	Asp-30	7.98	4.49	2.85, 3.09	
Ser-7	8.04	4.32	3.93, 4.13		Ile-31	8.19	3.69	1.90	CγH$_2$ 1.06
Leu-8	8.29	4.13	1.87	CγH 1.56					CγH$_3$ 0.71
				CδH$_3$ 0.83					CδH$_3$ 0.82
Glu-9	8.45	4.09	2.21	CγH$_2$ 2.44, 2.61	Trp-32	8.55	4.27	3.01, 3.31	2H 7.02
Ser-10	7.99	4.30	3.98, 4.09						4H 7.52
Leu-11	8.00	4.11	1.77	CγH 1.64					5H 6.97
				CδH$_3$ 0.79					6H 7.13
Asn-12	8.28	4.46	2.83	NH$_2$ 6.68, 7.49					7H 7.39
Asn-13	8.16	4.54	2.85, 2.89	NH$_2$ 6.78, 7.51					NH 9.60
Tyr-14	8.11	4.26	2.98, 3.03	2,6H 6.78	Arg-33	8.56	3.89	1.94, 2.03	CγH$_2$ 1.72, 1.92
				3,5H 6.69					CδH$_2$ 3.23
Phe-15	8.43	4.32	3.22, 3.10	2,6H 7.27					NH 6.25, 7.16
				3,5H 7.21	Asn-34	7.89	4.49	2.76, 2.86	NH$_2$ 6.75, 7.43
				4H 7.24	Trp-35	8.35	4.42	3.31	2H 7.10
Asn-16	8.16	4.73	2.89	NH$_2$ 6.74, 7.58					4H 7.42
Ser-17	8.04	4.43	3.93, 4.01						5H 7.07
Ser-18	8.06	4.40	3.84						6H 7.19
Gly-19	8.12	3.94							7H 7.42
Ile-20	7.65	4.12	1.85	CγH$_2$ 1.46					NH 9.71
				CγH$_3$ 0.90	Gln-36	8.04	3.79	1.79	CγH$_2$ 1.92
				CδH$_3$ 1.19					NH$_2$ 7.42
Asp-21	8.16	4.63	2.84		Lys-37	7.73	4.11	1.85	CγH$_2$ 1.45
Val-22	7.99	3.79	2.15	CγH$_3$ 0.98, 1.04					CδH$_2$ 1.68
Glu-23	8.30	4.12	2.16, 2.19	CγH$_2$ 2.47					CεH$_2$ 2.98
Glu-24	8.19	4.05	2.18	CγH$_2$ 2.40, 2.55	Asp-38	8.00	4.66	2.76, 2.85	
Lys-25	8.09	4.00	1.89	CγH$_2$ 1.34, 1.53	Gly-39	7.94	3.71, 3.81		
				CδH$_2$ 1.62					
				CεH$_2$ 2.90					
				NH$_3^+$ 7.27					

[a] Referenced with respect to internal DSS.

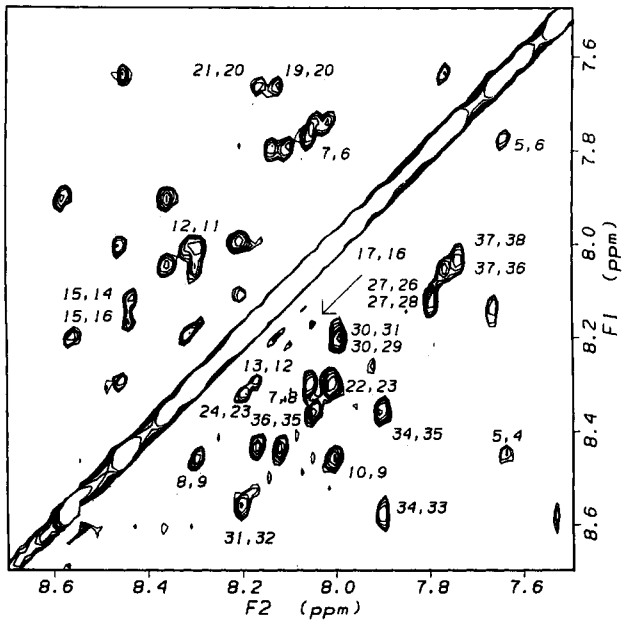

FIGURE 3: Amide proton region in the NOESY spectrum of MuIFNγ(1–39). The mixing time was 300 ms. The sequential d_{NN} connectivities are identified in the spectrum.

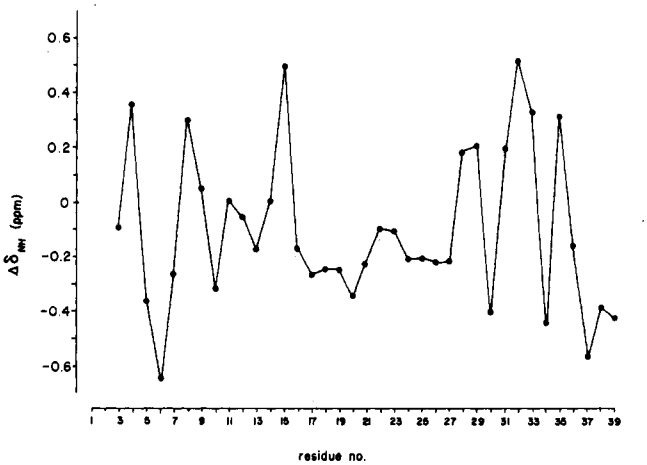

FIGURE 4: Deviation of the amide proton chemical shifts from the corresponding "coil" values for the individual amino acids in MuIFNγ-(1–39). The coil values were taken from Table 7 of Wishart et al. (1991). The text contains further discussion.

random-coil chemical shifts in water, whereas the former reflect the average values from secondary structures (including random coil) other than α-helices and β-sheets. Considering that the use of TFE in the solvent mixture may introduce a systematic change in the chemical shifts of amino acids compared to water alone as the solvent, it is perhaps not surprising that the "coil" values, which are in general smaller than the random-coil values, appear to provide a better reference set in our case. We have found that the former values were slightly more consistent with the results deduced from NOESY and vicinal coupling constant analysis.

Figure 4 shows a plot of the deviations of the amide hydrogen chemical shift values from the corresponding "coil" values

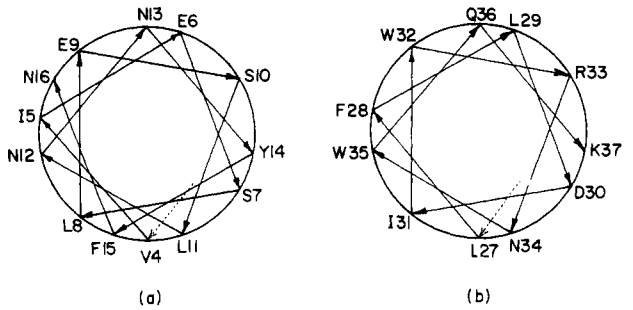

FIGURE 5: Helical wheel representation for regions 4–16 (a) and 27–38 (b) of MuIFNγ(1–39) showing the amphipathic nature of the A and B helices. Not included are residues 22–26 which are also part of the B helix.

reported in the work by Wishart et al. (1991).[2] The most striking feature of this figure is the apparent periodicity observed for residues 3–15 and residues 27–37. On the basis of observations from the published NMR data on different proteins (Kuntz et al., 1991), such a periodicity appears to be a characteristic of amphipathic helices where the hydrophobic residues tend to cluster on one side and the hydrophilic residues tend to cluster on the opposite side. This periodicity has been ascribed to a smooth bending of the helix axis due to stronger hydrogen bonds on the hydrophobic side and weaker bonds on the hydrophilic sides (Kuntz et al., 1991). In an amphipathic helix, the hydrophobic residues tend to show positive shifts, and the hydrophilic residues tend to show negative shifts compared to the coil values (Kuntz et al., 1991; Zhou et al., 1992). On the bais of this criterion, our studies suggest that MuIFNγ(1–39) is, in fact, characterized by three separate helical regions. Two sections, comprised of residues 3–15 and 27–37, show the expected periodicity characteristic of amphipathic helices; a short third α-helix composed of residues 22–27 is not amphipathic. That this is indeed the case is confirmed by the helical wheels shown in Figure 5. Figure 5a shows the helical wheel for residues 4–16 with the hydrophobic residues 5, 12, 8, 15, 4, 11, and 14 on one side and the hydrophilic residues 16, 9, 13, 6, and 10 on the other side. The second amphipathic helix is characterized by residues 27, 38, 31, 35, 28, 32, 36, and 29 on the hydrophobic side and residues 26, 30, 33, and 34 on the hydrophilic side. A third, short stretch of α-helix which is not amphipathic is characterized by residues 22–26. It is particularly gratifying that the amide proton chemical shift differences shown in Figure 4 are reasonably compatible with the location of the residues in the helical wheels depicted in Figures 5.

(*d*) *Other NOESY Contacts.* We have also observed several NOESY contacts which are indicative of additional conformational features beyond what have been described above. These involve side-chain–side-chain interactions of residues within the α-helices. No long-range NOESY contacts between the helical segments were observed, even at long mixing times (700 ms) and lower temperatures (5 °C).

It should be noted that the intact IFNγ exists as a dimer in aqueous solution. The synthetic fragment exhibited severe aggregation in aqueous solution which necessitated the use of TFE to dissolve the peptide. It is conceivable that the solvent interactions that discourage the intermolecular aggregation also discourage an interaction between the two helical segments. This suggestion is also consistent with the studies by Zhou et al. (1992) on an amphipathic peptide where, at concentrations above 25% (v/v), TFE actually discourages aggregation.

Structural Features of MuIFNγ(1–39) in Solution. On the basis of the above observations, we conclude that MuIFNγ-(1–39) assumes a helix–loop–helix conformation in solution. The loop region is formed by residues 16–21. This loop is flanked by two α-helices formed by residues 5–15 and 22–38. The N-terminal tripeptide (HGT) is probably poorly defined in its conformation as evidenced by the absence of any relevant NOESY contacts. No long-range NOESY contacts between the two helices were observed. It is likely that because of the presence of the loop region, MuIFNγ(1–39) exhibits a conformational manifold in which the relative orientation of the two helices shows considerable variability in solution. Such a situation is reasonable since tertiary interactions (including those between the two proteins in the dimer) that stabilize the relative arrangement of different helices in the native protein are absent in our studies. The XPLOR-based dynamical simulated annealing calculations resulted in the expected conformational manifold of helix–loop–helix structures.

It is instructive to compare the solution structure of the mouse IFNγ(1–39) with the conformation of the corresponding segments in the solution (Grzesiek et al., 1992) and crystal structures of human (Ealick et al., 1991) and rabbit (Samudzi et al., 1991) IFNγ dimer. We note that the mouse fragment has only about 35% sequence homology with respect to the corresponding segments in the human and rabbit sequences. Each monomeric unit in the intact dimeric protein is characterized by 6 helices (A–F and A′–F′) of which 2 helices (A and B) are contained in the N-terminal 40-residue region. In the crystal structure of the human protein, helix A is formed by residues 4–15, and helix B is formed by residues 28–36. In the solution structure of the intact human protein, the A helix is slightly larger (residues 5–17) while the B helix is smaller (residues 30–36) than is evident in the crystal structure. In the rabbit protein, residues 5–15 form the A helix while residues 28–33 form the B helix. That we see a slightly larger B helix in MuIFNγ(1–39) (i.e., residues 22–38) is not surprising since the first three residues in this helix (viz., V-22, E-23 and E-24) are α-helix-formers and, furthermore, TFE has a helix-stabilizing influence. In the crystal structure of HuIFNγ, the A and B helices are joined by a loop composed of residues 16–27. Weak electron density for this region suggested that this loop is disordered in the crystal structure (Ealick et al., 1991). In addition, helices A and B are not adjacent to each other in the crystal structure but are separated by the F′ helix from the second molecule in the symmetric dimer. Some minor conformational heterogeneity for residues 27 and 28 is suggested by the appearance of a very weak parallel set of resonances (from the 27′ and 28′ in the minor conformer) close to the amide TOCSY spectra of residues 27 and 28, and by the appearance of very weak exchange-mediated NOESY cross-peaks (Choe et al., 1991; Fejzo et al., 1991; Lee & Krishna, 1992) representing 27,28′ and 27′,28 connectivities in the amide NOESY spectra.

Our observation that the N-terminal tripeptide may not have an ordered structure is consistent with the CD data of Magazine and Johnson (1991), who reported that the α-helical content remained unchanged in the CD spectra of the 1–39 and 3–39 fragments. The observation that the MuIFNγ-(3–39) is also able to compete for receptor (Magazine & Johnson, 1991), and that the IFNγ lacking the first three residues produced by recombinant methods is also biologically active (Zavodny et al., 1988), suggests that these residues may not be involved in receptor interaction.

[2] We should also point out that Zhou et al. (1992) have also used "coil" values (and not random coil values) in their Figure 5A for an amphipathic helix in water/TFE mixtures.

Our findings concerning the solution structure of the IFNγ receptor binding peptide IFNγ(1–39) and the X-ray crystal structure data showing the lack of stable structure in the loop joining helices A and B (which is shorter than the one we observe here) suggest that this region of IFNγ can undergo structural changes when associated with receptor. Given the helix-forming tendencies of residues 22, 23, and 24 of IFNγ, this region of the loop, when associated with receptor, could possibly undergo a transition to a helix conformation that we observed with IFNγ(1–39) in 40% TFE. Future studies will involve determination of the bound conformation of labeled (^{15}N and ^{13}C) IFNγ(1–39) when complexed to soluble receptor (Griggs et al., 1992). This, in turn, may provide insight into the structural basis for activation of the receptor by IFNγ.

REFERENCES

Bax, A., & Davis, D. G. (1985) *J. Magn. Reson. 65*, 355–360.

Choe, B. Y., Cook, G. W., & Krishna, N. R. (1991) *J. Magn. Reson. 94*, 387–393.

Driscoll, P. C., Gronenborn, A. M., Beress, L., & Clore, G. M. (1989) *Biochemistry 28*, 2188–2198.

Ealick, S. E., Cook, W. J., Senadhi, V. K., Carson, M., Nagabhushan, T. L., Trotta, P. P., & Bugg, C. E. (1991) *Science 252*, 698–702.

Fejzo, J., Krezel, A. M., Westler, W. M., Macura, S., & Markley, J. (1991) *Biochemistry* **30**, 3807–3811.

Griggs, N. D., Jarpe, M. A., Pace, J. L., Russell, S. W., & Johnson, H. M. (1992) *J. Immunol. 149*, 517–520.

Grzesiek, S., Dobeli, H., Gentz, R., Garotta, G., Labhardt, A. M., & Bax, A. (1992) *Biochemistry 31*, 8180–8190.

Jarpe, M. A., & Johnson, H. M. (1990) *J. Immunol. 145*, 3304–3309.

Jarpe, M. A., & Johnson, H. M. (1993) *J. Interferon Res. 13*, 99–104.

Johnson, H. M. (1985) *Lymphokines 11*, 33–46.

Krishna, N. R., Sarathy, K. P., Huang, D. H., Stephens, R. L., Glickson, J. D., Smith, C. W., & Walter, R. (1982) *J. Am. Chem. Soc. 104*, 5051–5053.

Kuntz, I. D., Kosen, P. A., & Craig, E. C. (1991) *J. Am. Chem. Soc. 113*, 1406–1408.

Lee, W. T., & Krishna, N. R. (1992) *J. Magn.* Reson. *98*, 36–48.

Macura, S., & Ernst, R. R. (1980) *Mol. Phys. 41*, 95–117.

Magazine, H. I., & Johnson, H. M. (1991) *Biochemistry 30*, 5784–5789.

Magazine, H. I., Carter, M. J., Russell, J. K., Torres, B. A., Dunn, B. M., & Johnson, H. M. (1988) *Proc. Natl. Acad. Sci. U.S.A. 85*, 1237–1241.

Marion, D., & Wuthrich, K. (1983) *Biochem. Biophys. Res. Commun. 113*, 967–974.

Metzler, W. J., Hare, D. R., & Pardi, A. (1989) *Biochemistry 28*, 7045–7052.

Perkins, S. J. (1982) in *Biological Magnetic Resonance* (Berliner, L. J., & Reuben, J., Eds.) Vol. 4, pp 79–144, Plenum Press, New York.

Rance, M., Sorensen, O. W., Bodenhausen, G., Wagner, G., Ernst, R. R., & Wuthrich, K. (1983) *Biochem. Biophys. Res. Commun. 69*, 979–987.

Samudzi, C. T., Burton, L., & Rubin, J. R. (1991) *J. Biol. Chem. 266*, 21791–21797.

Wagner, G., Pardi, A., & Wuthrich, K. (1983) *J. Am. Chem. Soc. 105*, 5948–5949.

Wishart, D. S., Sykes, B. D., & Richards, F. M. (1991) *J. Mol. Biol. 222*, 311–333.

Wishart, D. S., Sykes, B. D., & Richards, F. M. (1992) *Biochemistry 31*, 1647–1651.

Wuthrich, K. (1986) *NMR of Proteins and Nucleic Acids*, Wiley-Interscience, New York.

Zavodny, P. J., Petro, M. E., Chiang, T., Narula, S. K., & Leibowitz, P. J. (1988) *J. Interferon Res. 8*, 483–494.

Zhou, N. E., Zhu, B., Sykes, B. D., & Hodges, R. S. (1992) *J. Am. Chem. Soc. 114*, 4320–4326.